Study on Alcoholysis of Waste PET and Its Application in Wood Modification

This work is licensed under a Creative Commons Attribution 4.0 International License

W. Xiang,[a] Z. Li,[a] B. Zhang,[a] H. Tang,[a,*] X. Yuan,[b] and T. Xu[a]

[a]Faculty of Chemical Engineering,
Kunming University of Science and Technology,
Kunming, Yunnan, China

[b]Ochemate Advanced Material Technologies Co,
Huzhou, Zhejiang, China

doi: https://doi.org/10.15255/CABEQ.2023.2197

Original scientific paper
Received: March 9, 2023
Accepted: January 25, 2024

Polyethylene terephthalate (PET), a thermoplastic polyester, is frequently used in plastic packaging such as bottles, films, and synthetic fibers. Due to its slow degradation in the natural environment, the accumulation of PET in large quantities poses a serious threat to the ecosystem. In this study, camphor pine wood was impregnated with these products by first alcoholyzing the waste PET, followed by the creation of a functional resin. The process of PET binary alcoholysis and unsaturated polyester (UPR) synthesis successfully incorporated certain characteristic groups from the PET raw material structure into the subsequent products of each stage, and cured them into a bulk unsaturated polyester with *p*-phenylene structure. The curing reaction primarily occurred in the carbon-carbon double bonds, according to the FTIR analysis of the PET raw material and the products at each stage. Under ideal conditions, the vacuum impregnation enhancement modification of camphor pine led to a 52.1 % increase in compressive strength and a decrease in water absorption from 103.8 % to 42 %, effectively enhancing the wood's compressive strength and resistance to water absorption.

Keywords
vacuum impregnation, wood alteration, unsaturated polyester, PET recycling

Introduction

Wood, comprising natural polymers such as cellulose, hemicellulose, and lignin, is an environmentally friendly material extensively utilized in various industries, including construction, furniture production, interior and outdoor decoration, and paper manufacturing. However, the availability of high-quality wood falls short of market demand due to historical overexploitation of natural forests and recent logging restrictions[1]. With inherent voids like cell cavities, gaps, and grain pores, wood exhibits a certain degree of porosity and permeability. Wood can be compressed or modified through physical or chemical methods, where chemical impregnation modification involves the infusion of functional resins into the wood's internal structure to improve its performance[2]. Fast-growing wood from plantations, with shorter development cycles, is scarcer than fast-growing wood from natural forests, which makes it easier to improve and modify fast-growing wood.

Leveraging wood's porous permeability, chemical impregnation modification fills gaps or triggers chemical reactions to embed specific functional components within the wood's internal structure, thereby enhancing its mechanical strength, dimensional stability, thermal stability, water absorption resistance, corrosion resistance, flame retardancy, light transmission, and other properties. Bliem *et al.*[3] utilized low molecular weight phenolic resin as impregnant and binder to enhance the tensile strength and hardness of spruce veneer. He et *al.*[4] impregnated wood with tung oil, significantly improving moisture absorption resistance and dimensional stability through oxidative and free radical polymerization within the wood.

Polyethylene terephthalate (PET), an industrialized linear thermoplastic resin, is produced through the ester exchange and direct esterification methods[5]. The main chain of PET contains a benzene ring, which enhances the polyester's mechanical strength and melting point, while ethylidene gives it flexibility. As a result, PET exhibits excellent chemical, physical, barrier, and optical transparency properties across a wide temperature range, finding extensive application in plastic packaging such as bottles, films, and synthetic fibers. Due to its tendency to accumulate in the environment after use and its slow disintegration in the ecosystem, "plastic pollution" poses significant environmental harm[6]. Thus, recycling PET waste has garnered

*Corresponding author: Email: thz9017@163.com

considerable attention, with physical, biological, and chemical recycling being the three primary methods.

Physical recycling, also known as mechanical recycling, involves converting recycled PET waste into new PET products through shredding, granulating, or physical mixing without altering the chain structure of PET molecules'[7]. Biological recycling is a process that breaks down PET into its individual molecules using microorganisms or degradation enzymes. PET molecular chains undergo changes during chemical recycling. Under specific reaction conditions and with the aid of degradation agents, the reversible equilibrium mechanism of the polyesterization reaction allows PET to transform into oligomers, terephthalic acid (TPA), ethylene glycol (EG), dimethyl terephthalate (DMT), bis(2-hydroxyethyl) terephthalate (BHET), and other products[8,9]. These products can then be used to create vital chemical raw materials like *p*-xylylenediamine[10] and 1,4-cyclohexanedimethanol[11], as well as to synthesize various polymers including PET[9,12], polyurethanes (PU)[13,14], unsaturated polyester resins (UPR)[15,16], alkyd resin[17], epoxy resin and its hardener[18], plasticizers[19], and composite additives[20–22], all exhibiting excellent performance.

The most promising approach to recycling waste PET involves diluting it into matching monomers or oligomers, which can then be utilized in the production of plastics and other high-tech products. PET diolysis is typically conducted at temperatures between 180 and 240 °C. Alcohololytic agents include ethylene glycol (EG), propylene glycol (PG), diethylene glycol (DEG), 1,4-butanediol (BDO), mono-dipropylene glycol (DPG), etc.[23] As illustrated in Fig. 1[24], the reaction is conducted in the presence of an ester exchange catalyst, the PET ester bond is broken, replaced by hydroxyl end groups, and the BHET monomer is produced as the final byproduct of complete depolymerization. By initially alcoholyzing waste PET with ethylene glycol (EG), followed by creating an unsaturated polyester resin and subsequently employing it to modify fast-growing wood, a symbiotic relationship between wood and waste PET was established. Under optimal experimental conditions for alcoholysis and UPR synthesis, successful impregnation into the wood's interior was achieved, resulting in enhanced compressive strength, thermal stability, and water absorption resistance of the wood.

Materials and methods

Industrial PET pellets, commercial 191-type resin (99 %), and Chinese Pinus sylvestris were all purchased from the market. Waste PET recycled material was obtained by recycling PET bottles. Ethylene glycol (EG, 99 %, code E) was procured from Guangdong Guanghua Technology Co. Zinc acetate dihydrate (99 %), sodium carbonate anhydrous (99 %), hydroquinone (99 %), and dibutyl phthalate (99 %) were purchased from Sinopharm Group Chemical Reagent Co. The Shanghai Maclean Biochemical Co., provided maleic anhydride (99 %), phthalic anhydride (99 %), styrene (St, 99 %, code S), methyl methacrylate (MMA, 99 %, code M), and benzoyl peroxide (BPO, 99 %, code B). Divinylbenzene (DVB, 80 %, code D) was purchased from Tianjin Baima Technology Co., and ethyl acetate (99 %) was sourced from Tianjin Zhiyuan Chemical Reagent Technology Co.

Waste PET and UPR in the ethylene glycol alcoholysis process

The PET packaging bottles were cleaned, cut into small square flakes (5 mm ×5 mm × 0.45 mm), dried, and stored in a desiccator. Ehylene glycol and catalyst were added into a three-necked flask, heated to 180 ℃, followed by the addition of waste PET recovery material (EG/PET = 8:1, molar ratio). The reaction temperature was maintained, condensation occurred, and reflux was initiated. The alcoholysis reaction was considered complete when all PET recovery material disappeared, and the resulting product became transparent and clear in color.

When the temperature of the PET alcoholysis system reduced to around 150 °C, maleic anhydride

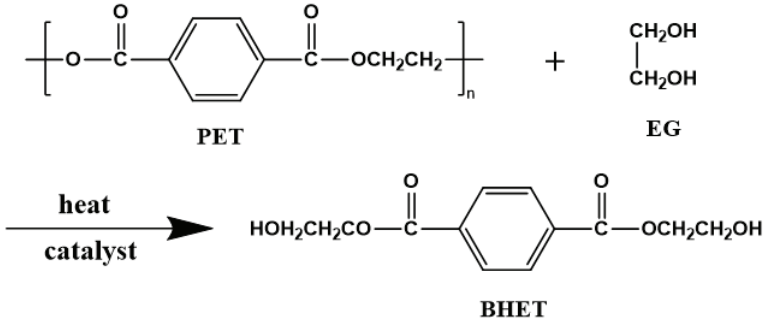

Fig. 1 – *Glycolysis of waste PET by EG*

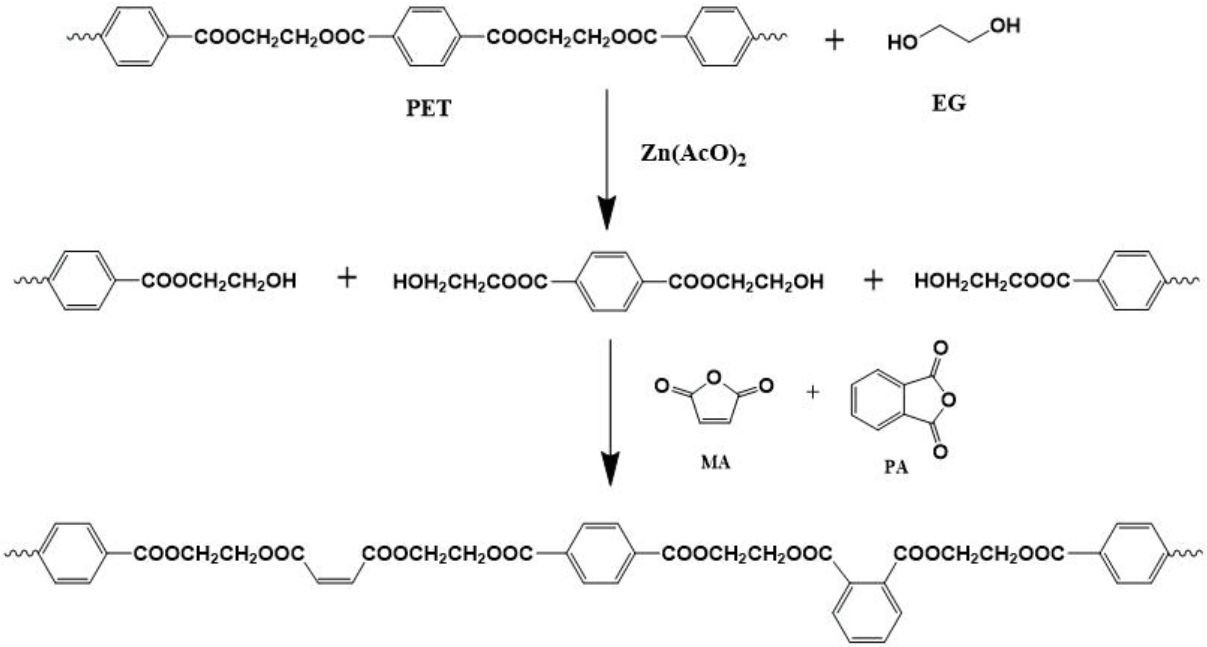

Fig. 2 – *Reaction diagram of EG alcoholysis PET and synthesis of UPR oligomer*

(MA) and phthalic anhydride (PA) (n_{PET+EG}:n_{MA+PA} = 1.2:1, n_{MA}:n_{PA} = 1:1) were added. The alcoholysis device was switched to reflux and distillation, stirring commenced, and the temperature was raised to 170–175 °C. The esterification reaction was initiated at this temperature, with control over the distillate steam temperature not exceeding 105 °C. Acid value was determined according to GB/T 6743-2008[25]. Once the acid value decreased to 135 mgKOH g^{-1}, the reaction temperature was raised to 190~200 °C for polycondensation reaction, upon which the acid value decreased to 50 mgKOH g^{-1}, and heating was stopped. When the reaction system's temperature decreased to 120 °C, 0.025 wt% of hydroquinone was added to the system. Fig. 2 depicts the reaction scheme for PET alcoholysis and UPR oligomer creation. When the temperature decreased to 90 °C, 20 wt% of styrene (St), 10 wt% of methyl methacrylate (MMA), and 2 wt% of divinylbenzene (DVB) were added. Stirring was stopped once the UPR oligomers were fully dissolved in the mixtures. In this study, the UPR oligomer combination is denoted as "EP-SMD". Table 1 provides a list of the article's code names along with their corresponding explanations.

Table 1 – *List of the article's codes and their definitions*

Code name	Definition
I-PET, PET	Industrial PET pellets, recycled PET trash
EP	Alcohol lysate products of the waster PET recycling material, after EG alcoholysis
EP-SMD	Blend UPR oligomer
EP-SMD-B	UPR following treatment with BPO as the catalyst
EP-SMD-B-Z	Wood that has been manipulated and cured

Determination of UPR oligomer viscosity

The viscosity of the combination of UPR oligomers dissolved in diluent/crosslinker was determined using an NDJ-1 rotary viscometer (Shanghai Precision Scientific Instrument Co.) in accordance with the procedure outlined in GB/T 7193-2008 [26].

Determination of UPR curing reaction activity

According to the method outlined in GB/T 7193-2008 [26], 10 g of UPR oligomer and a certain amount of BPO were mixed evenly and poured into a test tube. A thermocouple temperature probe was inserted into the center of the resin solution, and a constant temperature water bath was maintained at 80 ± 0.5 °C. The water bath level exceeded the resin liquid level, and the temperature was recorded every 10 seconds.

Waste PET-based UPR curing

UPR crosslinking and curing entail a free radical polymerization reaction, often requiring the involvement of initiators. In this experiment, organic peroxide initiators (mostly benzoyl peroxide BPO) were utilized to initiate the polymerization reaction at temperatures ranging from 60 to 80 °C.

Determination of curing degree of UPR

The soluble components in the cured UPR resin specimens were extracted with ethyl acetate close

to the boiling point temperature using a Soxhlet extractor, according to the regulations in GB/T 2576-2005 [27]. The insoluble fraction was considered as the cured resin. The degree of curing was determined using the following formula:

$$\alpha = \frac{m'}{m} \cdot 100\ \% \quad (1)$$

where m (g) is the mass of the specimen before extraction and m' (g) is the mass of the specimen after extraction.

Impregnation technique using waste PET-based UPR for camphor pine

Wood specimens of similar density (20 mm × 20 mm × 30 mm) were selected, vacuum dried at 103 ± 2 ℃ for 2 h to ensure absolute dryness, put into the impregnation bottle, and pre-vacuumized for 30 min. The UPR impregnation system with an initiator agent was then introduced into the bottle under –0.08 MPa pressure, not over the specimens. The pressure was maintained, and vacuum impregnation was conducted for 30 min. Subsequently, the specimens were impregnated again under normal pressure for 2 h to ensure complete impregnation[28]. The specimens were removed from the surface with filter paper after impregnation in order to remove any excess impregnation solution, and the mass of the specimens after impregnation was weighed. The specimens were then placed in the oven to cure under the predetermined curing conditions. After curing, the wood samples were weighed again, and further performance tests were conducted.

Determination of the impregnation rate and curing weight gain rate of the modified wood

Equation (2) was used to compute the impregnation rate IY of the wood impregnated with the UPR system, while equation (3) was used to calculate the curing weight gain rate WPG of (2):

$$\mathrm{IY} = \frac{W_2 - W_1}{W_1} \cdot 100\ \% \quad (2)$$

$$\mathrm{WPG} = \frac{W_3 - W_1}{W_1} \cdot 100\ \% \quad (3)$$

where W_1 is the mass in grams of the specimen of raw wood; W_2 is the mass in grams of the specimen of impregnated wood; and W_3 is the mass in grams of the specimen of cured wood.

Determination of the profile density of the modified wood

The profile density of the modified wood was determined using the pycnometer method. The wood specimens were cut into outer, middle, and inner chord cut profile sheets approximately 3 mm thick, parallel to the wood grain. These sheets were then sliced into strip specimens for analysis. Experimental steps included weighing the wood sample (m_1), weighing the mass of the pycnometer filled with distilled water (m_0), placing the wood sample into the water-filled pycnometer, wiping off any spilled water on the outer wall of the pycnometer, and weighing it (m_2).

$$\rho = \frac{m_1}{m_0 + \mathrm{m}_1 - m_2}\rho_0 \quad (4)$$

where, m_0 (g) is the mass of the pycnometer filled with water; m_1 (g) is the mass of the wood sample; m_2 (g) is the mass of the pycnometer containing wood samples and water; ρ_0 (g cm^{-3}) is the density of distilled water.

Determination of water resistance of the modified wood

According to the method outlined in GB/T 1934.1-2009 [29], the specimens were dried and weighed before being submerged in distilled water. Ensuring that they were submerged below the water surface by at least 50 mm, the container was securely covered. After 6 h, the specimens were weighed for the first time, followed by subsequent weighings after 1, 2, 4, and 8 nights. The water absorption rate, A, of the modified wood sample was calculated using the following formula:

$$A = \frac{m_n - m_0}{m_0} \cdot 100\ \% \quad (5)$$

where m_n (g) is the mass of the wood sample after water absorption; m_0 (g) is the mass of the wood sample when completely dry.

Determination of compressive strength along the grain of the modified wood

Utilizing a pressure testing machine (YAW-100D, Jinan Zhongluchang Testing Machine Manufacturing Co.) and following the procedure outlined in GB/T 1935-2009 [30], the compressive strength of the wood specimens along the grain was assessed. The test piece was placed in the center of the spherical movable support of the testing machine in the direction of the grain, with the loading speed was set to 0.5 KN s^{-1}. The failure load of the test piece was recorded, and the compressive strength (σ, MPa) along the grain of the modified wood specimen was calculated using the following formula:

$$\sigma = \frac{P_{\max}}{b \cdot t} \quad (6)$$

where, $P_{\max}$ (N) is the failure load; b (mm) is the width of the test piece; t (mm) is the length of the test piece.

Thermogravimetric analysis (TGA)

The modified wood was ground into powder specimens with particles smaller than 0.2 mm using a powder-making machine, while its thermal stability was assessed using a thermogravimetric analyzer (TGA-50, Shimadzu, Japan). The specimens were heated from room temperature to 800 °C at a rate of 10 °C min^{-1}, while the nitrogen flow rate was set to 20 mL min^{-1}. A comparative thermogravimetric analysis was carried out under identical conditions on log and UPR specimens.

FTIR spectroscopy of the modified wood

The wood specimens were cut parallel to the wood grain into outer, middle, and inner chordal slices approximately 2 mm thick. The FTIR (Spectrum Two, PerkinElmer, USA) characterization was conducted using ATR attenuated total reflection, with 8 scans performed and the test wavenumber range of the specimens set to 4000-400 cm^{-1}. The transverse coordinates of the spectra were expressed as transmittance.

Scanning electron microscopy of the modified wood (SEM)

To study the surface microscopic morphology, the log and modified wood specimens were cut into 5 mm × 5 mm × 2 mm chord-cut specimens from the chord direction. The specimens were gold sprayed to prevent charge buildup during characterization and fixed onto the SEM sample holder with conductive adhesive. Under vacuum, a thin metal layer was evenly sprayed on the surface of the wood samples to ensure full adhesion of the metal to the sample surface. Evaluation was performed at 20 kV accelerating voltage at 1000 and 5000 times magnification, respectively, using the TESCAN VEGA3 electron microscope from the Czech Republic.

Results and discussion

Process analysis of the glycolysis of waste PET and the synthesis of UPR

Glycolysis of waste PET and synthesis of UPR

The experiment investigated the influence of catalyst type (including Na_2CO_3 and $Zn(AcO)_2 \cdot 2H_2O$) and catalyst amount on the alcoholysis time. The results indicated that the alcoholysis time using 3 wt% Na_2CO_3 as the catalyst was similar to that using 2 wt% $Zn(AcO)_2 \cdot 2H_2O$ as the catalyst. Consequently, 2 wt% $Zn(AcO)_2 \cdot 2H_2O$ was chosen as the catalyst for glycol alcoholysis of waste PET.

Furthermore, we examined the effectiveness of alcoholysis in both industrial PET pellets and recovered waste PET. Industrial PET pellets were characterized as small oval cylinders (1.36 mm × 1.16 mm × 2.59 mm), while waste PET recycled material comprised small rectangular-shaped flakes (5 mm × 5 mm × 0.45 mm) cut from waste PET packaging bottles. Industrial PET pellets and waste PET recyclables exhibited specific surface areas of 8.19 $cm^2\ g^{-1}$ and 62.11 $cm^2\ g^{-1}$, respectively. The experimental results revealed that, under identical conditions (EP/PET = 8:1, 2.0 wt% $Zn(AcO)_2 \cdot 2H_2O$), the alcoholysis time of waste PET recycled material was 270 minutes, compared to 400 minutes for industrial PET particle material. The higher alcoholysis efficiency observed in waste PET recycled material can be attributed to its larger specific surface area, aligning with findings in existing literature[31,32]. The prefix "I" was added before the code of industrial PET recycled material and its subsequent products in order to differentiate them from waste PET recycled material and related subsequent goods.

FTIR analysis of PET raw materials and products at each stage

Fig. 3 presents the IR spectra of industrial PET pellets, waste PET recycled material, and the related alcoholysis products and UPR oligomer blends.

The IR spectra in Fig. 3 display typical absorption peaks for waste PET recycled material and industrial PET pellets. Alkyl chains manifest as double absorption peaks in the C–H stretching vibration range of 2960 to 2887 cm^{-1}, while C–O–C stretching vibration peaks at 1245cm^{-1} and 1100 cm^{-1} indicate the presence of ester groups. The para-substituted benzene ring is evident through the C–H out-of-plane bending vibration of the ring around 880 cm^{-1} and 730 cm^{-1}. The characteristic peak comparison revealed no difference between the chemical composition structures of industrial PET pellets and waste PET recycled materials, both exhibiting typical spectral band features of PET.

The spectra of PET alcoholysis products and UPR oligomers display absorption peaks in the PET structure at the same frequency positions, indicating successful introduction of distinctive groups from the PET feedstock structure into the subsequent stage products during the PET glycolysis and UPR synthesis processes.

Investigation of the curing characteristics of PET-based UPR

Impact of PET raw materials on the curing characteristics and degree of curing of UPR

The characteristics of the curing reactivity curves of the UPR systems synthesized from industrial PET pellets and waste PET recycled materials are compared in Fig. 4. The picture illustrates that

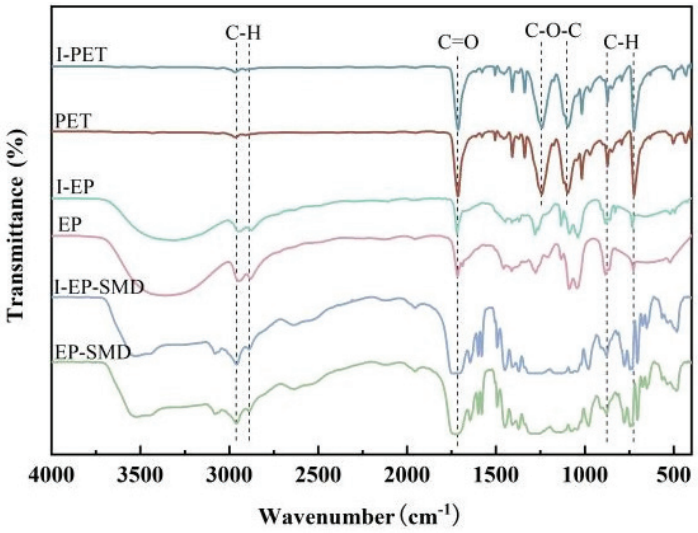

Fig. 3 – *Infrared spectra of PET raw materials and corresponding products*

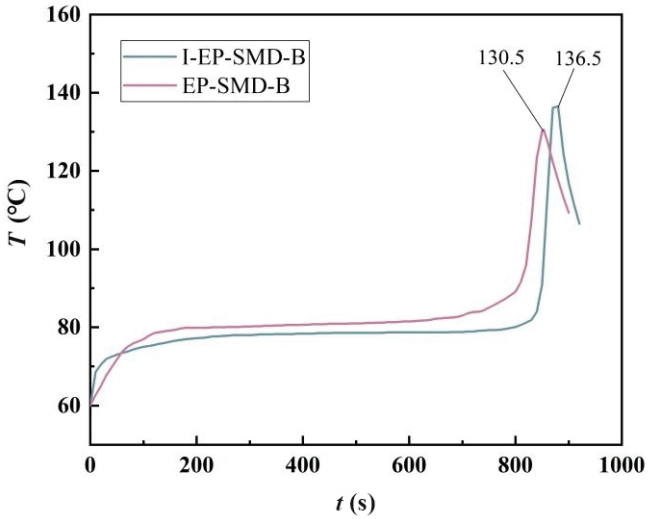

Fig. 4 – *Effect of PET raw materials on curing activity of UPR*

the curing reactivity curves of the UPR systems synthesized from PET recycled material and industrial material are generally similar, with the UPR curing reactivity of PET recycled material being marginally lower than that of PET industrial material.

Under the optimal initiator dosage of UPR curing (BPO dosage of 3 %) the UPR system synthesized from industrial PET pellets and waste PET recycled material was cured for 3 h, and the corresponding curing degree was measured in Table 2. It can be seen from the table that the curing degree of UPR synthesized from PET recycled material is slightly lower than that synthesized from PET industrial material, but still reaches more than 80 %, indicating that the curing ability of UPR synthesized from PET recycled material is also strong.

A comprehensive comparison of the effects of PET raw materials on the curing characteristics of UPR revealed that the curing characteristics of UPR synthesized from PET recycled materials were slightly inferior to those of UPR synthesized from PET industrial materials, most likely due to the aging and oxidation of recycled materials caused by light, heat, and abrasion during use, which slightly reduced the curing characteristics of the resulting UPR products. However, the UPR synthesized from PET recycled material has excellent curing reactivity and curing ability, allowing it to be utilized in the impregnation modification study of fast-growing wood.

Table 2 – *Comparison of curing degree of UPR synthesized from PET industrial material and recycled material*

Curing UPR system	Curing temperature (°C)	Initiator dosage (%)	Curing degree (%)
I-EP-SMD-B	80±2	3.0	86.0
EP-SMD-B	80±2	3.0	82.3

FTIR examination of cured UPR

Fig. 5 depicts the FTIR spectra of PET feedstock, UPR oligomer, and cured UPR triggered by BPO, from top to bottom. The free O–H stretching vibration absorption peak near 3500 cm^{-1} and the C=C stretching vibration absorption peak at 1645 cm^{-1} in the spectrum of UPR oligomer almost disappeared in the spectrum of cured UPR, which indicates that the end hydroxyl groups on the molecular chain of UPR oligomer will continue to react with the carboxyl groups during the curing process, and the small amount of water generated will evaporate during the high temperature curing process. The absence of the distinctive peak of the double bond suggests that UPR cross-linking happens primarily between the carbon-carbon double bond, and the double bond's free radical addition reaction converts the linear UPR to the bulk UPR.

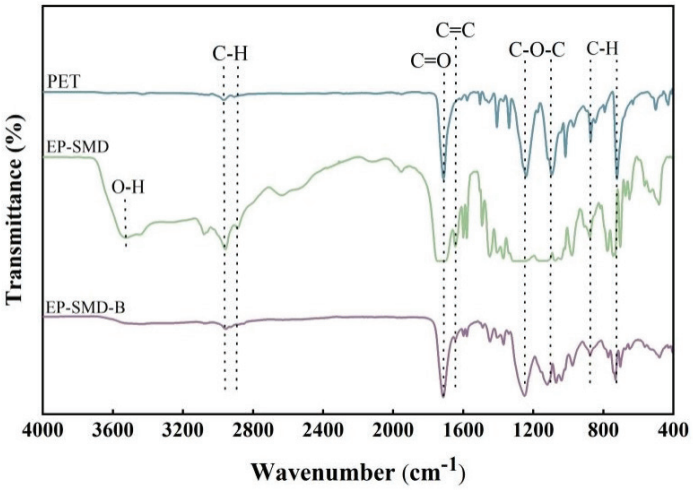

Fig. 5 – *Infrared spectra of PET and UPR products*

Research on the strengthening qualities of UPR-impregnated modified wood

Comparison of performance between modified wood and logs

According to Table 3 the impregnation rate and curing weight-gain rate of industrial PET-based UPR-impregnated modified wood were slightly higher than those of waste PET-based UPR impregnation system. Moreover, the impregnation rate and curing weight-gain rate of commercial 191-UPR-impregnated modified wood were higher. This difference can be attributed primarily to its much lower viscosity compared to the PET-based UPR system, resulting in relatively better liquidity and penetration capacity. The densities of the outer, middle, and inner profiles of the modified wood did not vary significantly; all were higher than the density of the original wood, and gradually decreased from the outer to the inner sections. This suggested that the UPR system successfully impregnated the wood's interior, while the impregnation effect from the outside to the interior gradually diminished. The wood's inherent material qualities contributed to uneven distribution of its own density, as well as to variations between the average density and profile density of the modified wood specimens.

Comparison of water absorption and compressive strength between modified wood and logs

Fig. 6 illustrates that the eight-day water absorption of camphor pine was 103.8 %, severely compromising its water and corrosion resistance requirements during further processing and application. However, the eight-day water absorption of the camphor pine modified by waste PET-based UPR impregnation was reduced to less than 42 %, significantly enhancing the wood's water absorption resistance to a level comparable to that of commercial UPR. Fig. 7 compares the compressive strength of virgin wood and modified wood. As mentioned previously, the impregnation weight-gain effect of waste PET-based UPR-impregnated modified wood was slightly lower than that of commercial UPR, but its compressive strength remained essentially the same as that of commercial UPR-impregnated modified wood.

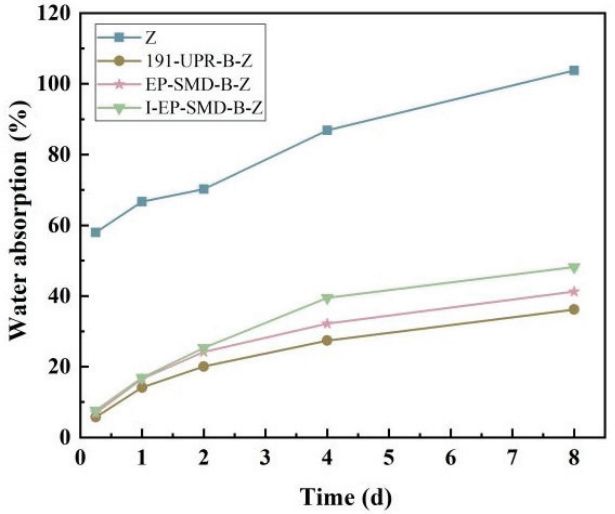

Fig. 6 – *Water absorption rate-time curves of modified woods*

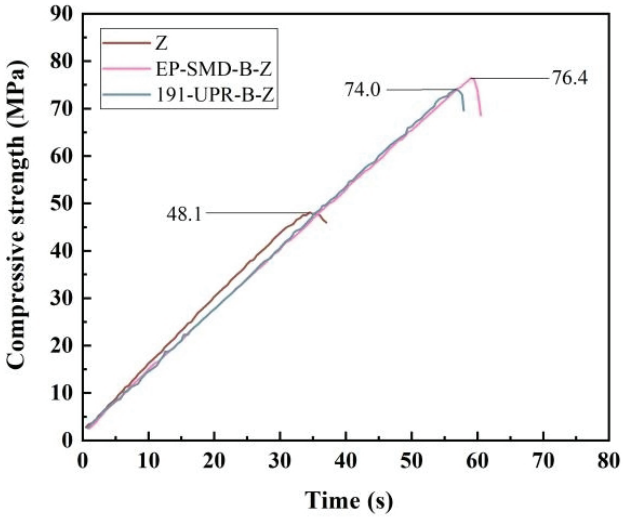

Fig. 7 – *Compressive strength-time curves of modified woods*

FTIR study of treated wood impregnated with UPR

Fig. 8 compares the FTIR spectra of the log chord section, inner, middle, and outer chord sections of the modified wood, and the waste PET-based UPR. The modified wood exhibited IR absorption characteristics of both logs and UPR. The IR characteristics of the inner chord section of the modified wood were closer to those of the logs, whereas the IR characteristics of the outer and middle chord sections of the modified wood were closer to those of the UPR.

Table 3 – *Performance comparison of Pinus sylvestris var. mongolica before and after impregnation*

UPR system	Viscosity (Pa s)	P_{log} (g cm^{-3})	$\rho_{Impregnated}$ (g cm^{-3})	Profile density			IY (%)	WPG (%)
				Outside	Middle	Inner		
I-EP-SMD	3.9	0.43	0.66	0.65	0.61	0.60	57.8	55.0
EP-SMD	4.2	0.47	0.68	0.64	0.62	0.60	47.9	45.3
191-UPR	0.6	0.42	0.67	0.72	0.65	0.62	63.3	59.8

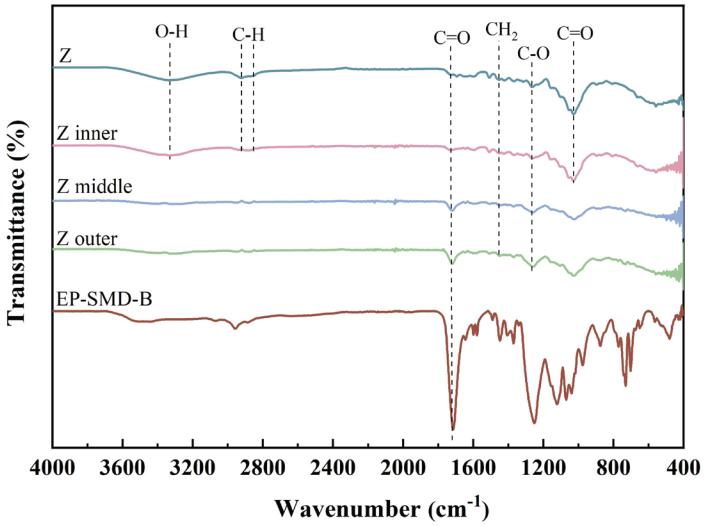

Fig. 8 – *Infrared spectra of modified woods*

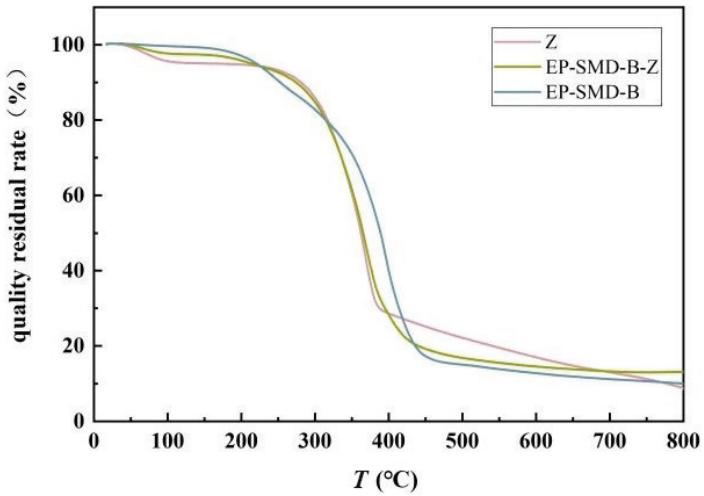

Fig. 9 – *Comparison of thermogravimetric curves between modified wood-logs and cured UPR*

Table 4 – *Comparison of relative contents of UPR in modified woods*

Modified wood sample name	Modified segment of camphor pine string		
	Outside	Middle	Inner
Ester carbonyl to $-CH_2$ transmittance ratio	0.94	0.96	1.02
Ester carbonyl to C–O transmittance ratio	1.02	1.01	1.06

To further examine the microscopic mechanism of the UPR-impregnated modified wood, the relative content of UPR in string section specimens was studied semi-quantitatively using the internal standard method of infrared spectroscopy. The $-CH_2$ in the lignin and polyxylose components of the wood, as well as the C–O in the lignin component, were less affected by other groups before to and after modification. Consequently, their IR characteristic absorption qualities remained stable, making them suitable as internal standard peaks. Using the ester carbonyl (C=O) near 1720 cm^{-1} as a reference and the $-CH_2$ and C–O peaks as internal standard peaks, the relative content of UPR in each profile of the modified wood was analyzed. The lower the ratio of ester carbonyl to the transmittance of internal standard peak, the higher the relative content of UPR. The transmittance ratio listed in Table 4, and comparison demonstrates a gradual decrease in the relative content of UPR from the outer to the inner chordal section of the modified wood, with the decreasing trend becoming relatively more pronounced as the inner part of the modified wood is approached. This is consistent with the pattern observed in Table 3 for the modified wood profile density.

Analysis of the thermal stability of UPR-impregnated modified wood (TGA)

The thermogravimetric curves in Fig. 9 illustrate significant weight loss processes as temperature increases for all the specimens. Table 5 presents the thermogravimetric study results of logs and modified wood based on the weight loss and weight-loss rates of the samples with temperature changes.

According to Table 5, the process of weight loss in both virgin and treated wood can be broken down into four stages. The first stage is the water loss stage[33], where the weight loss of the modified wood is lower than that of virgin wood. This indicates that under the same treatment conditions and preservation environment, the modified wood absorbed less water, implying higher water absorption resistance. This observation is consistent with the water absorption characteristics of the modified wood presented in Fig. 6, In the second phase, weight loss rates vary widely. In the temperature

Table 5 – *Thermogravimetric analysis results of logs and modified woods*

Sample name	Phase I		Phase II		Phase III		Phase IV	
	Temperature range (°C)	Weight-loss rate (%)	Temperature range (°C)	Weight-loss rate (%)	Temperature range (°C)	Weight-loss rate (%)	Temperature range (°C)	Weight-loss rate (%)
Z	23~121	4.48	121~216	0.86	216~436	73.34	436~800	7.32
EP-SMD-B-Z	23~115	2.89	115~250	4.89	250~465	72.89	465~800	5.03

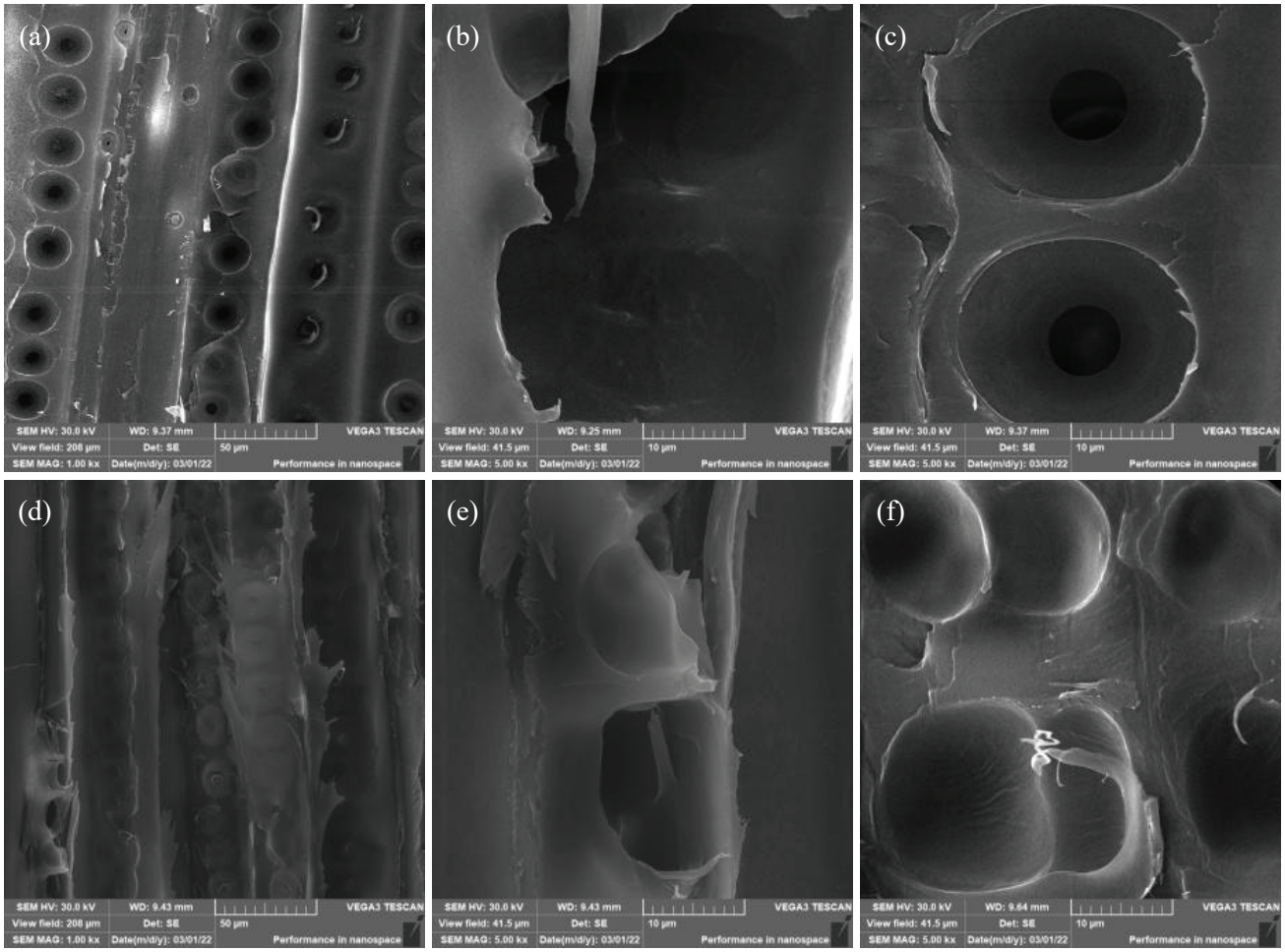

Fig. 10 – *The SEM pictures of pinus sylvestris log (a, b, c) and waste PET based UPR impregnated modified pinus sylvestris samples (d, e, f)*

range of 121~216 °C, which corresponds to the micro-weight loss stage, the mass of the logs remained relatively constant; the weight loss rate of the modified wood was 4.89 % in the temperature range of 115~250 °C, primarily due to the poor thermal stability of the few uncured UPR oligomers in the impregnation system and evaporation of uncured molecules, which caused weight loss first. The third stage is thermal breakdown, the primary stage of log and modified wood weight loss. The weight loss of logs was 73.34 % in the temperature range of 216~436 °C, primarily attributed to the pyrolysis of cellulose and hemicellulose[34]; the weight loss of modified wood was 72.89 % in the temperature range of 250~465 °C, indicative of the mixed pyrolysis process of the wood's cellulose and hemicellulose, and the cured UPR impregnation system. The fourth stage is the charring stage, during which the residual components in the logs and modified wood continue to slowly pyrolyze until charring, resulting in minimal weight loss of the specimens.

From Fig. 9, it is evident that there was 8.5 % remaining residue in the logs, 9.9 % remaining residue in the cured UPR, and 13.2 % remaining residue in the modified wood. In terms of mass residual rate, the thermal stability of modified wood was slightly better than that of the logs.

Scanning electron microscopy analysis of the UPR-impregnated modified wood (SEM)

Fig. 10 presents the scanning electron micrographs of the inner chord sections of both the logs and modified camphor wood. In the inner chord sections of the logs, there was no discernible adhesion of conduit molecules, wood fibers, or wood ray cavities. Additionally, the grain pore openings and cavities were open, providing a pathway and location for the waste PET-based UPR system to infiltrate the cell cavities, interstices, grain pores, and other voids. In contrast, the inner chordal section of the modified wood was partially filled and adhered with translucent resin in the cell cavities of duct molecules, wood fibers, and wood rays. Moreover, the grain pore openings were nearly completely occluded by resin. These observations indicate that the UPR system successfully impregnated the wood without detriment to the wood's microstructure. Figs. 10(a), 10(b), and 10(c) depict scanning elec-

tron microscopy images of the inner chord section samples of camphor pine logs, while Figs. 10(d), 10(e), and 10(f) represent scanning electron microscopy images of inner chord section samples of modified camphor pine. Figs. 10(a) and 10(d) are magnified 1000 times, whereas Figs. 10(b), 10(c), 10(e), and 10(f) are magnified 5000 times.

Grain holes serve as pathways for the movement of water and other liquids within the wood's microstructures. The UPR impregnation system seals the majority of the wood's grain pores, thereby reducing the modified wood's permeability, and significantly enhancing its resistance to water absorption. Within wood structure, wood fibers (in broadleaf wood) and tubular cells (in coniferous wood) provide primary mechanical support. The UPR system fills, adheres to the walls of these cells, and crosslinks and cures them, thereby enhancing the compressive strength of the modified wood.

Conclusion

This paper investigates the synthesis of UPR through the binary alcoholysis of waste PET and its subsequent application in the enhancement modification of fast-growing wood. Employing a systematic and progressive research approach, we identified the optimal process scheme and modification mechanism for the impregnation of fast-growing wood with waste PET-based UPR. The vacuum impregnation enhancement of camphor pine under optimized conditions resulted in a 52.1 % increase in compressive strength, and a reduction in water absorption from 103.8 % to 42 %, thereby significantly enhancing the wood's compressive strength and resistance to water absorption. Profile density measurements and FTIR analysis of the waste PET-based UPR-impregnated modified wood revealed a gradual decrease in the relative content of UPR from the outer chordal section to the inner chordal section. This indicated that the UPR impregnation mode was dominated by lateral penetration, with decreasing permeability from the outer to the inner section of the wood. Thermogravimetric analysis demonstrated a slight improvement in the thermal stability of the PET-based unsaturated resin impregnated modified wood. SEM observations revealed that the microstructure of the modified wood remained intact. Furthermore, the UPR impregnation system effectively filled and adhered to various components of the wood structural tissue, including duct molecules, wood fibers, tubular cells, and wood rays. This cross-linking and curing process occluded the grain pores in the cell walls, thereby enhancing water absorption resistance and mechanical strength of the fast-growing wood.

References

1. *Hoganson, H. M., Meyer, N. G.,* Constrained optimization for addressing forest-wide timber production, Curr. For. Rep. **1** (2015) 33. doi: https://doi.org/10.1007/s40725-015-0004-x
2. *Acosta, A. P., Barbosa, K. T., Amico, S. C., Missio, A. L., Delucis, R. d. A., Gatto, D. A.,* Improvement in mechanical, physical and biological properties of eucalyptus and pine woods by raw pine resin in situ polymerization, Ind. Crops Prod. **166** (2021) 113495. doi: http://dx.doi.org/10.1016/J.INDCROP.2021.113495
3. *Bliem, P., Konnerth, J., Fromel-Frybort, S., Gartner, C., Mauritz, R., van Herwijnen, H. W. G.,* Influence of drying and curing parameters on phenol-formaldehyde impregnated wood veneers, J. Adhes. **96** (2020) 253. doi: https://doi.org/10.1080/00218464.2019.1657015
4. *He, Z., Qian, J., Qu, L., Yan, N., Yi, S.,* Effects of Tung oil treatment on wood hygroscopicity, dimensional stability and thermostability, Ind. Crops Prod. **140** (2019) 111647. doi: https://doi.org/10.1016/j.indcrop.2019.111647
5. *Ho, P. S., Kim, S. H.,* Poly (ethylene terephthalate) recycling for high value added textiles, Fash. Text. **1** (2014) 1. doi: https://doi.org/10.1186/s40691-014-0001-x
6. *Taniguchi, I., Yoshida, S., Hiraga, K., Miyamoto, K., Kimura, Y., Oda, K.,* Biodegradation of PET: Current status and application aspects, ACS Catal. **9** (2019) 4089. doi: https://doi.org/10.1021/acscatal.8b05171
7. *Leng, Z., Padhan, R. K., Sreeram, A.,* Production of a sustainable paving material through chemical recycling of waste PET into crumb rubber modified asphalt, J. Clean Prod. **180** (2018) 682. doi: https://doi.org/10.1016/j.jclepro.2018.01.171
8. *Rahimi, A., García, M. J.,* Chemical recycling of waste plastics for new materials production, Nat. Rev. Chem. **1** (2017) 409. doi: https://doi.org/10.1038/s41570-017-0046
9. *Thiounn, T., Smith, R. C.,* Advances and approaches for chemical recycling of plastic waste, J. Polym. Sci. **58** (2020) 1347. doi: https://doi.org/10.1002/pol.20190261
10. *Raheem, A. B., Noor, Z. Z., Hassan, A., Abd Hamid, M. K., Samsudin, S. A., Sabeen, A. H.,* Current developments in chemical recycling of post-consumer polyethylene terephthalate wastes for new materials production: A review, J. Clean Prod. **225** (2019) 1052. doi: https://doi.org/10.1016/j.jclepro.2019.04.019
11. *Westhues, S., Idel, J., Klankermayer, J.,* Molecular catalyst systems as key enablers for tailored polyesters and polycarbonate recycling concepts, Sci. Adv. **4** (2018) 9669. doi: https://doi.org/10.1126/sciadv.aat9669
12. *Tournier, V., Topham, C. M., Gilles, A., David, B., Folgoas, C., Moya-Leclair, E., Kamionka, E., Desrousseaux, M. L., Texier, H., Gavalda, S., Cot, M., Guemard, E., Dalibey, M., Nomme, J., Cioci, G., Barbe, S., Chateau, M., Andre, I., Duquesne, S., Marty, A.,* An engineered PET depolymerase to break down and recycle plastic bottles, Nature **580** (2020) 216. doi: https://doi.org/10.1038/s41586-020-2149-4
13. *Espinoza Garcia, K., Navarro, R., Ramirez-Hernandez, A., Marcos-Fernandez, A.,* New routes to difunctional macroglycols using ethylene carbonate: Reaction with bis-(2-hydroxyethyl) terephthalate and degradation of poly(ethylene terephthalate), Polym. Degrad. Stabil. **144** (2017) 195. doi: https://doi.org/10.1016/j.polymdegradstab.2017.08.018

14. *Zhou, X., Wang, C., Fang, C., Yu, R., Li, Y., Lei, W.,* Structure and thermal properties of various alcoholysis products from waste poly(ethylene terephthalate), Waste Manage. **85** (2019) 164.
doi: https://doi.org/10.1016/j.wasman.2018.12.032
15. *Abdullah, N. M., Ahmad, I.,* Potential of using polyester reinforced coconut fiber composites derived from recycling polyethylene terephthalate (PET) waste, Fiber. Polym. **14** (2013) 584.
doi: https://doi.org/10.1007/s12221-013-0584-7
16. *Karpati, L., Szarka, G., Hartman, M., Vargha, V.,* Oligoester and polyester production via acido-alcoholysis of PET waste. Period, Polytech.-Chem. Eng. **62** (2018) 336.
doi: https://doi.org/10.3311/PPch.11513
17. *Atta, A. M., El-Ghazawy, R. A., El-Saeed, A. M.,* Corrosion protective coating based on alkyd resins derived from recycled poly (ethylene terephthalate) waste for carbon steel, Int. J. Electrochem. Sci. **8** (2013) 5136.
18. *Atta, A. M., El-Kafrawy, A. F., Aly, M. H., Abdel-Azim, A. A. A.,* New epoxy resins based on recycled poly(ethylene terephthalate) as organic coatings. Prog. Org. Coat. **58** (2007) 13.
doi: https://doi.org/10.1016/j.porgcoat.2006.11.001
19. *Shukla, S. R., Kapadi, P. U., Mhaske, S. T., Mali, M. N., More, A.,* Synthesis of a secondary plasticizer for poly(vinyl chloride) by recycling of poly(ethylene terephthalate) bottle waste through aminolytic depolymerization, J. Vinyl Addit. Technol. **23** (2017) 152.
doi: https://doi.org/10.1002/vnl.21494
20. *Leng, Z., Padhan, R. K., Sreeram, A.,* Production of a sustainable paving material through chemical recycling of waste PET into crumb rubber modified asphalt, J. Clean Prod. **180** (2018) 682.
doi: https://doi.org/10.1016/j.jclepro.2018.01.171
21. *Sogancioglu, M., Yucel, A., Yel, E., Ahmetli, G.,* Production of epoxy composite from the pyrolysis char of washed PET wastes, Energy Procedia. **118** (2017) 216.
doi: https://doi.org/10.1016/j.egypro.2017.07.022
22. *Leng, Z., Sreeram, A., Padhan, R. K., Tan, Z.,* Value-added application of waste PET based additives in bituminous mixtures containing high percentage of reclaimed asphalt pavement (RAP), J. Clean Prod. **196** (2018) 615.
doi: https://doi.org/10.1016/j.jclepro.2018.06.119
23. *George, N., Kurian, T.,* Recent developments in the chemical recycling of postconsumer poly(ethylene terephthalate) waste, Ind. Eng. Chem. Res. **53** (2014) 14185.
doi: https://doi.org/10.1021/ie501995m
24. *Sinha, V., Patel, M. R., Patel, J. V.,* Pet waste management by chemical recycling: A review, J. Clean Prod. **18** (2010) 8.
doi: https://doi.org/10.1007/s10924-008-0106-7
25. CNOOC Changzhou Paint & Chemicals Research Institute. Plastics (Polyester Resins) and Paints and Varnishes (Binders) -- Determination of Partial Acid Value and Total Acid Value. GB/T 6743-, Administration of Quality Supervision, Inspection and Quarantine of People's Republic of China; Standardization Administration of China, 2008.
26. General Administration of Quality Supervision, Inspection and Quarantine of the People's Republic of China. Test methods for unsaturated polyester resins. GB/T 7193-, China National Standardization Administration, 2008.
27. China Building Materials Industry Association. Test Method for Insoluble Matter Content of Resin Used in Fiber Reinforced Plastics. GB/T 2576-, General Administration of Quality Supervision, Inspection and Quarantine of the People Republic of China, China National Standardization Administration Committee, 2005.
28. *Ma, Q., Zhao, Z., Yi, S., Wang, T.,* Modification of fast-growing Chinese Fir wood with unsaturated polyester resin: Impregnation technology and efficiency, Results Phys. **6** (2016) 543.
doi: https://doi.org/10.1016/j.rinp.2016.08.017
29. Institute of Chinese Academy of Forestry Timber Industry. Method for Determination of the Moisture Content of Wood. GB/T 1934-, Administration of Quality Supervision, Inspection and Quarantine of People's Republic of China; Standardization Administration of China, 2009.
30. Method of Testing in Compressive Strength Parallel to Grain of Wood. GB/T 1935-, Administration of Quality Supervision, Inspection and Quarantine of People's Republic of China; Standardization Administration of China, 2009.
31. *Wang, Q., Lu, X., Zhou, X., Zhu, M., He, H., Zhang, X.,* 1-Allyl-3-methylimidazolium halometallate ionic liquids as efficient catalysts for the glycolysis of poly (ethylene terephthalate), J. Appl. Polym. Sci. **129** (2013) 3574.
doi: https://doi.org/10.1002/app.38706
32. *Al-Sabagh, A. M., Yehia, F. Z., Eissa, A.-M. M. F., Moustafa, M. E., Eshaq, G., Rabie, A.-R. M., ElMetwally, A. E.,* Glycolysis of poly(ethylene terephthalate) catalyzed by the Lewis base ionic liquid (Bmim)(OAc), Ind. Eng. Chem. Res. **53** (2014) 18443.
doi: https://doi.org/10.1021/ie503677w
33. *Azizi, K., Moraveji, M. K., Najafabadi, H. A.,* Characteristics and kinetics study of simultaneous pyrolysis of microalgae *Chlorella vulgaris*, wood and polypropylene through TGA, Bioresour. Technol. **243** (2017) 481.
doi: https://doi.org/ 10.1016/j.biortech.2017.06.155
34. *TranVan, L., Legrand, V., Jacquemin, F.,* Thermal decomposition kinetics of balsa wood: Kinetics and degradation mechanisms comparison between dry and moisturized materials, Polym. Degrad. Stabil. **110** (2014) 208.
doi: https://doi.org/10.1016/j.polymdegradstab.2014.09.004